ARTICLES

Dynamics of CHFClBr and CDFClBr Inside a Thiomethylated Cryptophane, Studied by $^{19}F-^{1}H$ CSA-DD Cross-Correlated Relaxation and ^{2}H Quadrupolar Relaxation Measurements

Jeanne Crassous* and Sabine Hediger

Laboratoire de Chimie (UMR 5532 CNRS/ENS), Ecole Normale Supérieure de Lyon, 46 Allée d'Italie, F-69364 Lyon Cedex 07, France

Received: May 5, 2003

The host−guest complexation of bromochlorofluoromethane (CHFClBr) and bromochlorodeuteriofluoromethane (CDFClBr) by a chiral thiomethylated cryptophane (cryptophane-E-$(SCH_3)_6$) was studied by fluorine NMR. Fluorine NMR T_1 experiments were performed on the {CHFClBr@cryptophane-E-$(SCH_3)_6$} system. They revealed the presence of $^{19}F-^{1}H$ CSA-DD cross-correlated relaxation, which was found to be more efficient inside the host cavity. The measurement of $^{19}F-^{1}H$ CSA-DD cross-correlated relaxation rates at two different magnetic field strengths allowed the determination of the correlation time τ_C of CHFClBr outside ($\tau_C = 0.27$ ns) and inside the cryptophane ($\tau_C = 0.62-0.78$ ns). These correlation times were confirmed by the measurement of the deuterium quadrupolar relaxation time T_q in the {CDFClBr@cryptophane-E-$(SCH_3)_6$} system. The two methods were in very good agreement and showed that the substrate was slowed upon complexation.

Introduction

Since 1981, cryptophanes have been an important topic in the field of supramolecular chemistry and more particularly in the host−guest complexation of small tetrahedral molecules. These studies were mainly achieved by Collet and co-workers.[1] Cryptophanes are constituted of two cone-shaped fragment molecules named cyclotriveratrylenes (CTV), linked with three bridges, of the most common type alkyloxy (see Figure 1). Such molecules are known to possess a cavity that is able to complex small guest molecules such as quaternary ammonia[2] and halogenomethanes[3] and noble gases such as xenon.[1,4] These guests are accommodated into the molecular cavity of the cryptophane through windows whose size depends on the length of the alkyloxy bridges and on the peripheral substitution (i.e., hydrogen, methoxy, and thiomethoxy). Many efforts have been made to understand the general features of the complexation process, both experimentally[4] and theoretically.[5] The question of the dynamics of the guest molecule inside the cavity of the cryptophane was addressed by several groups as well. For example, the dynamics of $CHCl_3$ inside cryptophane-E has been studied by Wipff and co-workers using computational calculations.[6] They found that the lifetime of each orientation of the bound guest varied from 20 to 60 ps. Kowalewski and co-workers have studied the same inclusion complex by NOE and carbon-13 T_1 relaxation experiments. Their analysis led to the conclusion of the presence of a strong dynamic coupling between the bound chloroform molecule and its host cryptophane-E.[7] A very different result was obtained in a similar study for dichloromethane in cryptophane-E. In this complex, the motion of the guest was found to be weakly coupled to the motion of the host.[8]

Historically, cryptophanes were "taylor-made" in order to discriminate the two enantiomers of one of the smallest chiral molecules, namely, bromochlorofluoromethane (CHFClBr, **5**). Chiral cryptophane-A (**1**) and later on cryptophane-C (**2**) were thus respectively synthesized in 1981[9] and in 1985,[10] by Collet and co-workers. Although cryptophane-A, with six peripheral methoxy groups, had too small windows to accommodate CHFClBr, cryptophane-C, with only three peripheral methoxy groups, showed a good chiral discrimination of CHFClBr, as was observed by proton NMR (nuclear magnetic resonance) spectroscopy, with a fast chemical exchange on the NMR time scale.[10]

Up to now, to our knowledge, the enantioselective recognition of CHFClBr by cryptophane-C[10,5a] has been the only case of complexation of a chiral molecule in the cryptophanes chemistry. We were therefore interested in other hosts able to differentiate between the two chiral forms of CHFClBr because such chiral systems may give additional knowledge about the complexation process, in terms of thermodynamics, kinetics, and dynamics of the chiral guest inside the chiral cryptophane. We present here the results obtained for the complex of CHFClBr (**5**) and CDFClBr (**6**) with cryptophane-E-$(SCH_3)_6$ (**4**), a thiomethylated analogue of cryptophane-E.[11] The dynamics of CHFClBr inside the cryptophane was studied using cross-correlated relaxation between the ^{19}F chemical-shift anisotropy (CSA) and the fluorine-proton dipolar interaction (DD). Deuterium quadrupolar relaxation, measured by means of fluorine NMR, was found to

* To whom correspondence should be addressed. Fax: +33 4 72 72 84 83. Tel: +33 4 72 72 87 33. E-mail: jeanne.crassous@ens-lyon.fr.

10.1021/jp0305685 CCC: $25.00 © 2003 American Chemical Society
Published on Web 11/11/2003

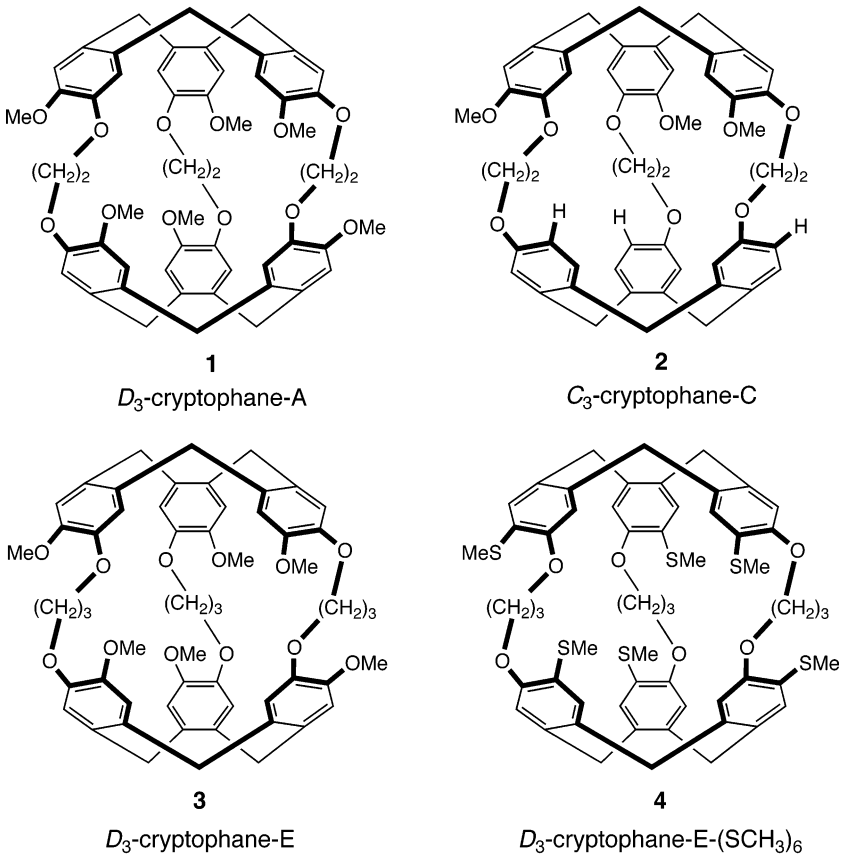

Figure 1. Some D_3 or C_3 symmetrical chiral cryptophanes.

be adequate as well for the study of the motion of CDFClBr inside the cavity of the cryptophane.

General Features of Complexation

Thiomethylated cryptophanes have recently revealed interesting complexation properties in comparison with their oxygenated analogues, as was exemplified by Garcia et al., who studied the complexation of $CHCl_3$ by cryptophane-E (**3**) and E-$(SCH_3)_6$ (**4**).[11] Although both cryptophane-E and E-$(SCH_3)_6$ have similar molecular cavity sizes, the main structural modification from E to E-$(SCH_3)_6$ is the obstruction of the host's windows due to the bigger size of the sulfur atoms. Moreover, the overall negative charges in the aromatic rings are decreased in the thiomethylated cryptophane. This results in an important slowdown of the complexation kinetics, as demonstrated by the half time values (0.55 s for $CHCl_3$ and host **3** versus 24 min for $CHCl_3$ and host **4**), and the equilibrium association constants (600 M^{-1} for $CHCl_3$ and host **3** versus 240 M^{-1} for $CHCl_3$ and host **4**).

The difference in the complexation properties of cryptophanes **3** and **4** was even more pronounced for the guest CHFClBr. As revealed by proton NMR, both hosts (±)-**3** and (±)-**4** exhibit complexation of (±)-CHFClBr. Indeed, proton NMR spectra given in Figure 2 show two highly up-shielded doublets (the splitting of the resonances in doublets is due to the $^1H-^{19}F$ J coupling) which correspond to the diastereomeric complexes and their corresponding mirror-images.[12] The complexation involves two equilibrium processes described in Figure 3. Figure 4 displays the fluorine NMR spectra: with both cryptophanes, signals corresponding to free and complexed CHFClBr are present, indicating a slow exchange on the NMR time scale. With cryptophane-E, the two fluorine signals corresponding to the diastereomeric complexes are however equally shielded, leading to two unresolved doublets, with the splitting coming from the $^{19}F-^1H$ scalar J coupling (Figure 4a). On the opposite, in the case of cryptophane E-$(SCH_3)_6$, the ^{19}F spectrum shows two well resolved doublets, corresponding to the diastereomeric complexes, up-shielded by respectively 1.53 ppm for Cpx1,F and 1.69 ppm for Cpx2,F, with respect to the signal of the free CHFClBr (Figure 4b). It is the first time that such discrimination is observed by ^{19}F NMR in a cryptophane inclusion complex. The reason for the different chemical shifts observed by ^{19}F NMR between the diastereomeric complexes 1 and 2 cannot be explained by the complexation process itself. It may come from the different chemical environment seen by the two enantiomers of CHFClBr inside the cavity in the presence of the sulfur heteroatoms. This result makes thiomethylated cryptophanes a new series of great importance in the recognition of chiral halogenomethanes.

Equilibrium association constants K were derived from the determination of the concentrations of the host and the guest molecule, obtained from the relative intensities in the proton NMR spectra (within an error of about 10%). We found values of $K = 100$ M^{-1} for Cpx1,H and $K = 108$ M^{-1} for Cpx2,H in the case of CHFClBr in host **3** (small enantioselective recognition) and $K = 10$ M^{-1} for both Cpx1,H and Cpx2,H in the case of CHFClBr and host **4** (no enantioselective recognition). As for the complexation of $CHCl_3$,[11] the association constant is much lower for host **4** compared to that for host **3**. Moreover, the influence of the size of the guest (by means of its van der Waals radius) on the complexation has been studied earlier. It was shown in the case of cryptophane-E that CHFClBr is less recognized than $CHCl_3$, because of its smaller size. In fact, among a series of halogenomethanes, $CHCl_3$ fits best in the cavity of cryptophane-E.[1]

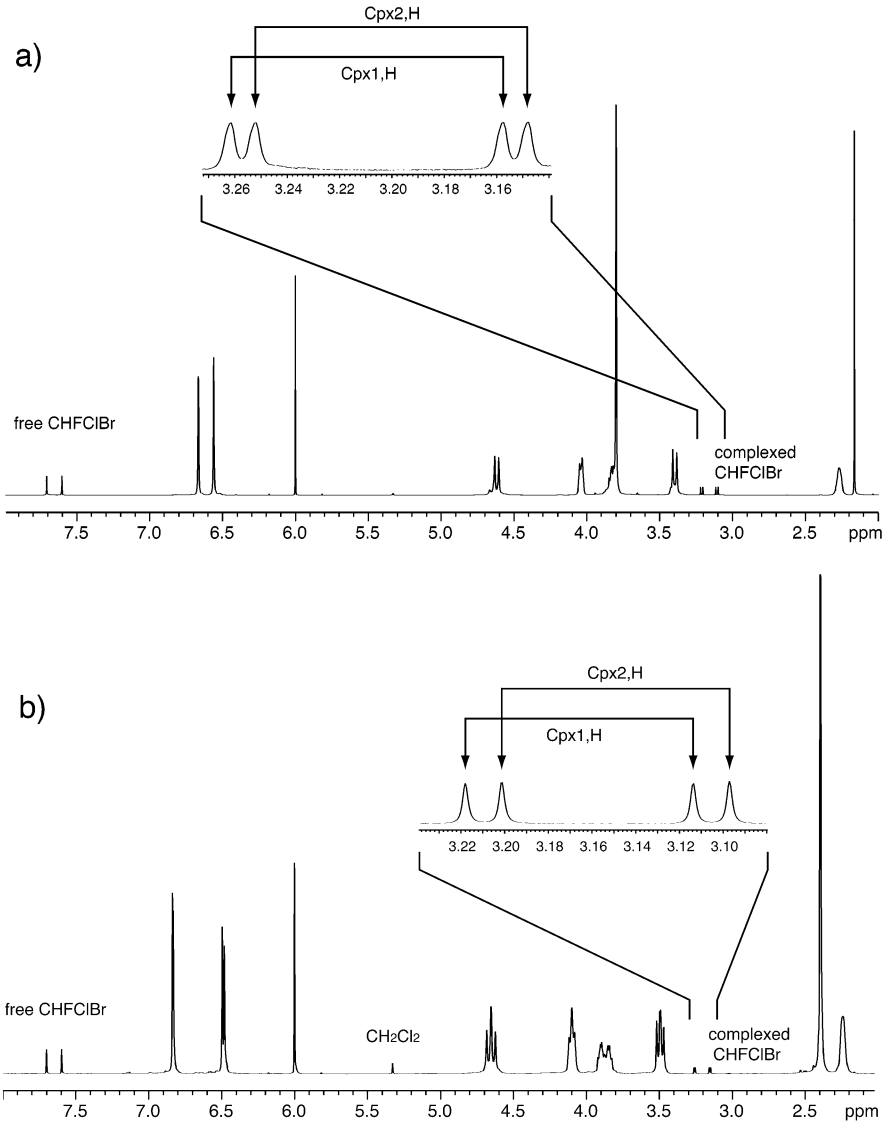

Figure 2. ^{1}H NMR spectra at a magnetic field of 11.74 T and a temperature of 298 K. (a) Complexation of (±)-CHFClBr by (±)-cryptophane-E. (b) Complexation of (±)-CHFClBr by (±)-cryptophane-E-$(SCH_3)_6$. In both parts, the signals corresponding to the two diastereomeric complexes are expanded.

$$\text{host} + \text{CHFClBr} \underset{}{\overset{K_1}{\rightleftharpoons}} \text{Cpx1 (down-shielded diastereomer)}$$

$$\text{host} + \textit{ent}\text{-CHFClBr} \underset{}{\overset{K_2}{\rightleftharpoons}} \text{Cpx2 (up-shielded diastereomer)}$$

$$K_1 = \frac{[\text{Cpx1}]}{[\text{host}]\cdot[\text{CHFClBr}]} \qquad K_2 = \frac{[\text{Cpx2}]}{[\text{host}]\cdot[\textit{ent}\text{-CHFClBr}]}$$

Figure 3. Equilibria involved in the complexation process of the two enantiomers of CHFClBr with a chiral host (with a certain defined configuration).

Isotope Effects on the Chemical Shifts (IECS)

The sensitivity of the ^{19}F chemical shift to the chemical environment is illustrated by the isotope effect observed in the NMR signal of CHF^{35}ClBr and CHF^{37}ClBr. These species are present in respective proportions of 76% and 24%, and lead in the ^{19}F spectrum to two peaks with slightly different chemical shifts (see Figure 4). The respective intensity of these peaks reflects the respective isotope abundance. The IECS[13] was found to be 6.6 ppb for the free haloform and about 6 ppb for the bound guest. In the case of the bound guest, the broader signals prevent one from properly distinguishing the isotopes.

Fluorine T_1 and CSA-DD Cross-Correlated Relaxation Measurements

The relaxation behavior of the NMR signal is very informative for the study of molecular dynamics. Most generally, NMR relaxation can be separated into different types depending on the mechanism responsible for the decay of the signal:[14] for example dipole−dipole (DD), chemical shift anisotropy (CSA) (for nuclei such as ^{15}N, ^{19}F, or ^{13}C), quadrupolar (for quadrupole nuclei such as ^{14}N or ^{2}H), paramagnetic (for example when O_2 is present in the NMR tube), scalar, or spin-rotation relaxation. To extract dynamic information, assumptions about the principal relaxation mechanisms and the type of motion have to be made. In the case of the complexation of CHFClBr, the fluorine nucleus seems to be a good probe for a relaxation study, having a spin 1/2 and a high gyromagnetic ratio. However, both its CSA and dipolar coupling to the proton are large and have to be taken into account for the interpretation of the ^{19}F relaxation. Moreover, an impact of the nearby quadrupole nuclei (Cl and Br) via scalar relaxation of the second kind cannot be excluded.

Fortunately, the measurement of the fluorine longitudinal relaxation time T_1 in our complexes has revealed a differential

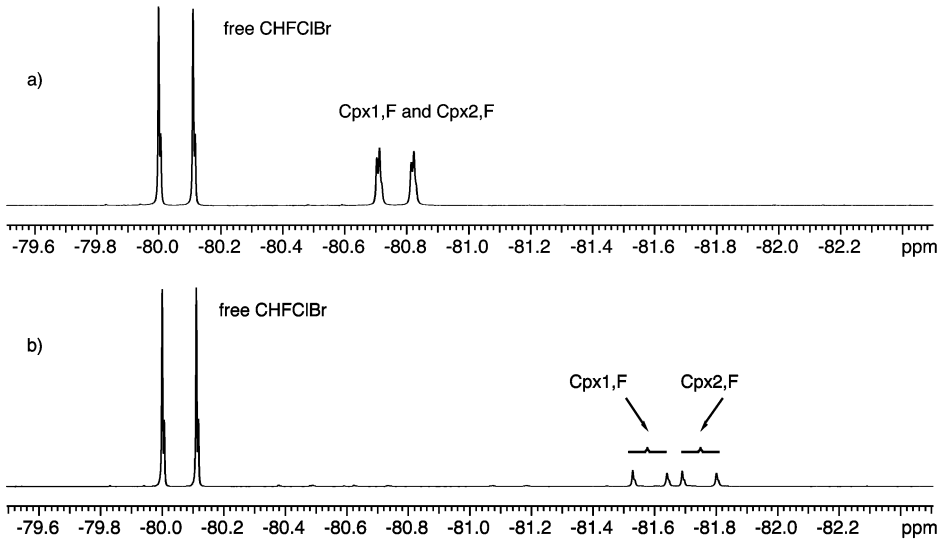

Figure 4. ^{19}F NMR spectra at a magnetic field of 11.74 T and a temperature of 298 K. (a) Complexation of (±)-CHFClBr by (±)-cryptophane E. (b) Complexation of (±)-CHFClBr by (±)-cryptophane-E-$(SCH_3)_6$.

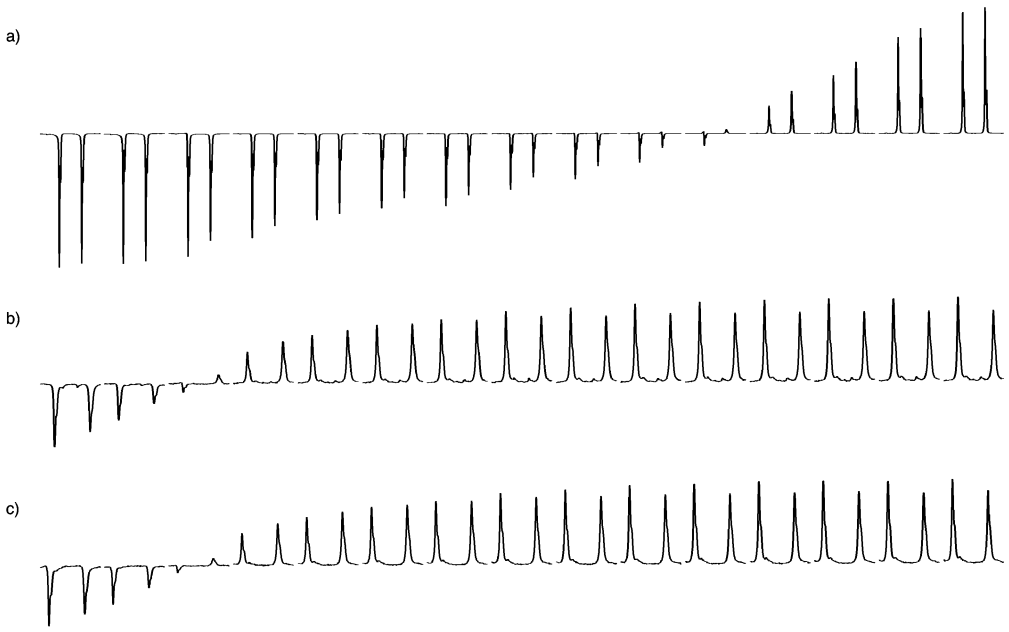

Figure 5. Relaxation behavior of the different ^{19}F lines observed in the inversion−recovery experiment for the complexation of (±)-CHFClBr by (±)-cryptophane-E-$(SCH_3)_6$. (a) free CHFClBr signal, (b) Cpx1,F signal, (c) Cpx2,F signal. This measurement was performed at 11.74 T and 298 K.

relaxation behavior of the two components of the doublet (the splitting is due to scalar J coupling with the proton) for the signals of both the free and complexed CHFClBr (see Figure 5). This kind of differential relaxation is undoubtedly caused by cross-correlated relaxation between the ^{19}F CSA and the ^{19}F−^{1}H DD interaction. Fluorine-proton CSA-DD cross-correlation has already been observed by Dorai et al. in several fluorinated benzenes.[15] Following their treatment, the fluorine longitudinal relaxation in the absence of chemical exchange is described by the equation of motion

$$\frac{\mathrm{d}}{\mathrm{d}t}\vec{M}(\mathbf{t}) = -\Gamma[\vec{M}(t) - \vec{M}_0] \qquad (1)$$

where the vector $\vec{M}(\mathbf{t})$ denotes the magnetization at time **t** and $\vec{M}_0$ is its equilibrium value. As we want to focus, in the case of CHFClBr, on the cross-correlated relaxation between the fluorine CSA and fluorine−proton dipolar interaction, the spin-system can be reduced to two weakly coupled spins H and F. The relevant modes of eq 1 are linear combinations of the fluorine and proton populations. For our system, the rate equation can be written as

$$\frac{\mathrm{d}}{\mathrm{d}t}\begin{bmatrix}\langle 1\rangle\\ \langle F_z\rangle\\ \langle H_z\rangle\\ \langle 2F_zH_z\rangle\end{bmatrix} = -\begin{bmatrix}0 & 0 & 0 & 0\\ 0 & \rho_F & \sigma_{FH} & \Delta^F_{FH}\\ 0 & \sigma_{FH} & \rho_H & \Delta^H_{FH}\\ 0 & \Delta^F_{FH} & \Delta^H_{FH} & \rho_{FH}\end{bmatrix}\begin{bmatrix}\langle 1\rangle\\ \langle \Delta F_z\rangle\\ \langle \Delta H_z\rangle\\ \langle \Delta 2F_zH_z\rangle\end{bmatrix} \qquad (2)$$

where the mode $\langle 1\rangle$ is the total sum of the populations, the single-spin order modes $\langle F_z\rangle$ and $\langle H_z\rangle$ are the total magnetizations of the corresponding spins, and $\langle 2F_zH_z\rangle$ is the two-spin order. ρ_F, ρ_H, and ρ_{FH} are the self-relaxation rates ($1/T_{1,F}$, $1/T_{1,H}$, and $1/T_{1,FH}$, respectively), and σ_{FH} is a relaxation rate that

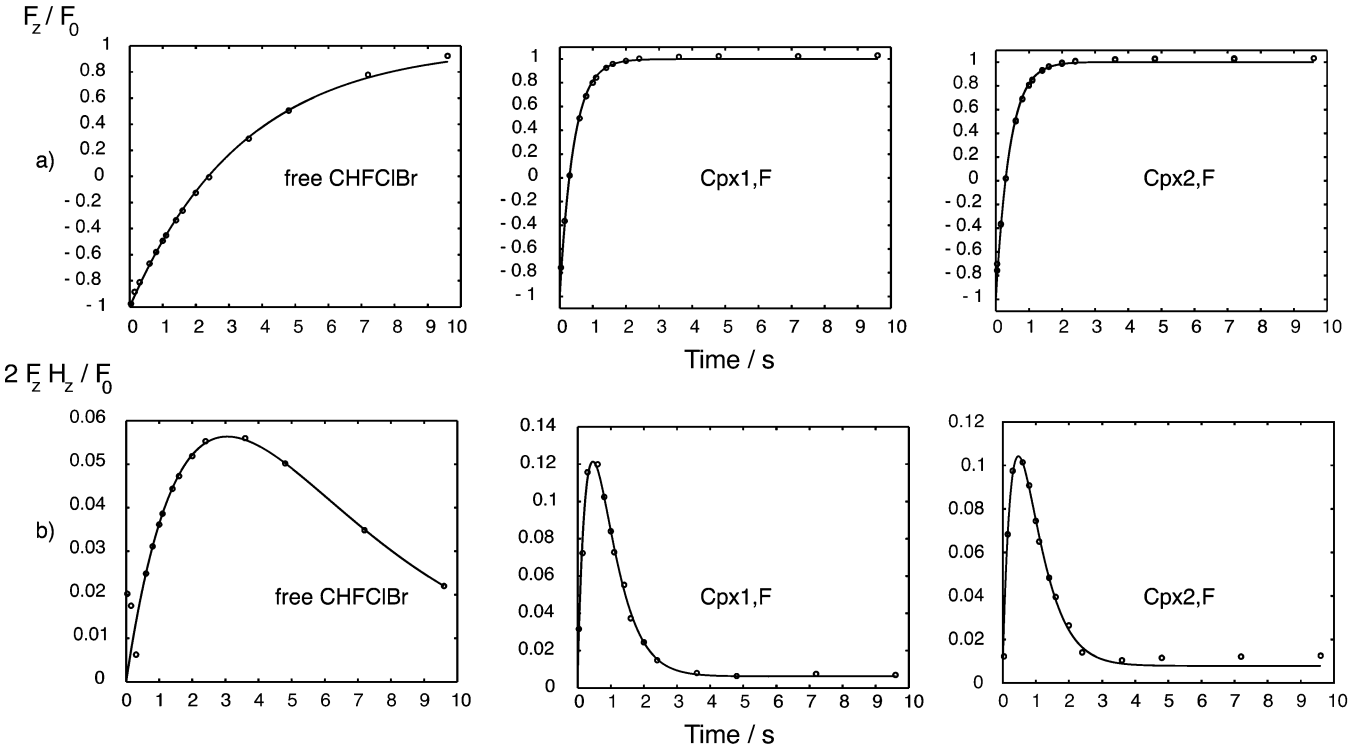

Figure 6. Evolution of the one-spin order (a) and two-spin order (b) components of the different ^{19}F line intensities obtained in the inversion recovery experiment of Figure 5 for the complexation of (±)-CHFClBr by (±)-cryptophane-E-$(SCH_3)_6$. The dots are the experimental values. The straight lines are the best fitting curves.

interconverts the single-spin order modes $\langle F_z\rangle$ and $\langle H_z\rangle$ (NOE effect). Δ^{F}_{FH} and Δ^{H}_{FH} are relaxation rates that interconvert single-spin and two-spin order. They have their origin in CSA-(i)−DD(ij) cross-correlated relaxation. It is interesting to note that, under conditions of proton decoupling, cross-relaxation (NOE and CSA-DD) is removed, leading to a monoexponential behavior of the fluorine longitudinal relaxation. However, such an approach was not possible on our spectrometer, which has only one high-frequency channel (^{1}H/^{19}F).

In an inversion−recovery experiment where the ^{19}F magnetization is inverted and detected at different relaxation times t, the build-up of the signal reflects the evolution of single-spin order $\langle F_z\rangle$ and two-spin order $\langle 2F_zH_z\rangle$. Besides an in-phase signal corresponding to the evolution of $\langle F_z\rangle$ with time, there is a build-up of an anti-phase doublet corresponding to the evolution of $\langle 2F_zH_z\rangle$. This leads to unequal relaxation for the two components of the doublet, and therefore to different signal intensities after the 90° detection pulse (Figure 5). The evolution of single-spin and two-spin order can be studied separately by decomposing the ^{19}F signal in an in-phase and an anti-phase contribution. In principle, the evolution of the fluorine signal has to be analyzed by solving the coupled equation of motion of eq 2, leading to a non-monoexponential behavior of both the in-phase and anti-phase component. However, as we are only interested in the cross-correlated relaxation rate Δ^{i}_{ij} given by the initial rate of the two-spin order build-up, a phenomenological approach is shown to be sufficient.

For the complex of CHFClBr in host **4**, the evolution of all three ^{19}F signals (one for the free CHFClBr and two for the two diasterotopic complexes of CHFClBr with **4**) obtained from an inversion−recovery experiment is given in Figure 5, whereas the separate evolution of the single-spin and two-spin orders is depicted in Figure 6. The chemical exchange is for this complex much slower than the NMR relaxation time T_1 (the rate constant of the chemical exchange is estimated to be of the same order of magnitude as in the case of $CHCl_3$)[11] and can therefore be ignored. The recovery of single-spin order could be very well fitted for all three signals with the monoexponential function

$$\langle F_z\rangle(t) = F_0\left[1 - 2\exp\left(-\frac{t}{T_1}\right)\right] \qquad (3)$$

The fact that the evolution of $\langle F_z\rangle$ is essentially monoexponential implies that the evolution of the single-spin order is dominated by the self-relaxation rate $\rho_F = 1/T_1$, the cross-correlation effects being negligible ($\rho_F \gg \sigma_{FH}, \Delta^{F,H}_{FH}$). The build-up and decay of two-spin order could be fitted with a phenomenological double-exponential function

$$\frac{\langle 2F_zH_z\rangle(t)}{F_0} = A\left[1 - \exp\left(\frac{-t}{T_{\text{build-up}}}\right)\right]\exp\left(\frac{-t}{T_{\text{decay}}}\right) \qquad (4)$$

The CSA-DD cross-correlated relaxation rate Δ^{F}_{FH} can then be obtained from the first derivative of $\langle 2F_zH_z\rangle(t)/F_0$ at $t = 0$ (initial rate approximation)

$$\Delta^{F}_{FH} = A/T_{\text{build-up}} \qquad (5)$$

This study was performed for the complex {CHFClBr@cryptophane-E-$(SCH_3)_6$} at two different magnetic field strengths corresponding to fluorine resonance frequencies of 468.4 and 188.2 MHz. The results of the numerical fits for the time evolution of single-spin ($\langle F_z\rangle(t)/F_0$) and two-spin ($\langle 2F_zH_z\rangle(t)/F_0$) order modes for each of the three ^{19}F signals are summarized in Tables 1 and 2. As clearly illustrated in Figure 6, CHFClBr relaxes more rapidly when complexed inside the cavity of the cryptophane. The build-up of two-spin order is more than 1 order of magnitude faster in the complex, resulting from a more efficient CSA-DD cross relaxation.

TABLE 1: Fit Results of the Evolution of Fluorine Longitudinal Magnetization at 468.4 MHz

	T_1/ [s]	A	$T_{build-up}$/ [s]	T_{decay}/ [s]	offset[a]	Δ^F_{FH}/ [s^{-1}]
free CHFClBr	3.42	0.28	5.58	4.07		0.05
Cpx1,F	0.42	2.23	3.30	0.50	0.006	0.68
Cpx2,F	0.42	1.80	3.25	0.51	0.008	0.55

[a] For a proper fitting of the anti-phase component, a small offset had to be added to eq 4.

TABLE 2: Fit Result of the Evolution of Fluorine Longitudinal Magnetization at 188.3 MHz

	T_1/ [s]	A	$T_{build-up}$/ [s]	T_{decay}/ [s]	offset[a]	Δ^F_{FH}/ [s^{-1}]
free CHFClBr	4.22	0.09	3.12	4.63		0.03
Cpx1,F	0.69	2.79	3.27	0.63	−0.012	0.85
Cpx2,F	0.71	1.90	2.53	0.65	−0.025	0.75

[a] For a proper fitting of the anti-phase component, a small offset had to be added to eq 4.

Determination of the Correlation Time τ_C from CSA-DD Cross-Correlated Relaxation Rates

The cross-correlated relaxation rate Δ^F_{FH} of longitudinal magnetization is proportional to the static magnetic field $\mathbf{B}_0$ and to the spectral density function of the molecular motion $J(\omega)$ at the Larmor frequency of the fluorine spin[16]

$$\Delta^F_{FH} \propto \mathbf{B}_0 \cdot J(\omega_F) \tag{6}$$

The proportionality factor contains information about the magnitude of the chemical shift anisotropy (in ppm), the dipolar interaction (e.g., H−F distance), and the relative orientation of the CSA and dipolar tensors. If we consider the simple case of CHFClBr isotropically tumbling in the cryptophane cavity,[17] eq 6 can be written as

$$\Delta^F_{FH} \propto \mathbf{B}_0 \left(\frac{\tau_C}{1 + \omega_F{}^2 \tau_C{}^2} \right) \tag{7}$$

with τ_C the correlation time of the molecular tumbling. Interestingly, the ratio X of Δ^F_{FH} rate constants measured at two different magnetic field strengths becomes independent of the ^{19}F CSA and ^{19}F−^{1}H dipolar interaction strength and relative orientation. The correlation time τ_C can then be obtained

$$X = \frac{\Delta^F_{FH,1}}{\Delta^F_{FH,2}} \frac{\mathbf{B}_{0,2}}{\mathbf{B}_{0,1}} = \frac{1 + \omega_{F,2}{}^2 \tau_C{}^2}{1 + \omega_{F,1}{}^2 \tau_C{}^2}$$

$$\Rightarrow \tau_C = \sqrt{\frac{1 - X}{X\omega_{F,1}{}^2 - \omega_{F,2}{}^2}} \tag{8}$$

Taking for Δ^F_{FH} the numerical values of Tables 1 and 2, $\omega_{F,1}/2\pi = 468.4$ MHz, $\omega_{F,1}/2\pi = 188.3$ MHz, and 0.4 for $\mathbf{B}_{0,2}/\mathbf{B}_{0,1}$, a correlation time of $\tau = 0.27$ ns was found for the free CHFClBr, $\tau_C = 0.62$ ns for Cpx1,F and $\tau_C = 0.78$ ns for Cpx2,F. As expected, the binding decreased the mobility of CHFClBr. Moreover, these values for the guest are in agreement with the results obtained by Kowalewski et al.[7] for $CHCl_3$ and cryptophane-E. Indeed, they obtained a τ_C value of 0.5 ns by considering the motion of $CHCl_3$ inside the cryptophane's cavity and a global τ_C of 0.67 ns when the host−guest system was considered as a single molecule. The authors also found a substantial order parameter and concluded that the van der Waals interaction was "highly anisotropic, behaving as a strong directional bond". The fact that the same order of magnitude was found for our system shows that the determination of the correlation time from CSA-DD cross-correlated relaxation measurements is rather reliable. We show in the next part that the same results are obtained from ^{2}H relaxation rate constants.

Deuterium T_q Relaxation Measurements

The principal relaxation mechanism for the deuterium spin is the quadrupolar relaxation, which can be used to study the dynamics of a deuterated molecule. For this reason, the complexation process of racemic CDFClBr (±)-**6** by thiomethylated cryptophane-E-$(SCH_3)_6$ (±)-**4** was studied by ^{19}F NMR in $C_2D_2Cl_4$ at 298 K. The quadrupolar relaxation of the ^{2}H spin has an impact on the resonance line shape of the coupled fluorine spin (scalar relaxation of the second kind).[20] The deuterium quadrupolar relaxation time T_q in CDFClBr can therefore be obtained indirectly from a line shape analysis of the fluorine resonance. The correlation time τ_C is subsequently calculated from T_q. Such a study was performed at a magnetic field strength of 11.74 T corresponding to a ^{19}F resonance frequency of 468.4 MHz.

The ^{19}F NMR spectrum, depicted in Figure 7, shows distinct signals for the free and the bound CDFClBr (together with the signals corresponding to free and bound CHFClBr also present in the sample). The signal of the free species is a triplet ($J = 8$ Hz), whereas two up-shielded singlets are observed for the two diastereomeric complexes. This fact is well explained by what is called scalar relaxation of the second kind: the NMR line shapes of a spin $I = 1/2$ coupled to a spin $I' = 1$ is either a triplet or a singulet, depending on the quadrupolar relaxation time T_q.[18,19] When the quadrupolar relaxation is slow compared to the J coupling between both spins, the splitting due to the J coupling is resolved in the spin 1/2 spectrum. As T_q becomes shorter, the splitting disappears progressively, and a single line is finally obtained for the spin 1/2 resonance when the quadrupolar relaxation becomes much faster than the time scale of the J coupling. The line shapes are well reproduced by the following equation:[20]

$$I(x) = \frac{45 + \eta^2(5x^2 + 1)}{225x^2 + \eta^2(34x^4 - 2x^2 + 4) + \eta^4(x^6 - 2x^4 + x^2)} \tag{9}$$

with $x = (\omega_i - \omega)/J$ and $\eta = 5T_qJ$. $I(x)$ represents the intensity of the resonance line as a function of the frequency ω. ω_i and J are the resonance frequency of the observed nucleus (fluorine in our case) and the coupling constant ($J_{DF} = 8$ Hz), respectively.

The resonance line shapes of free and bound CDFClBr (Figure 7b) could be fitted using eq 9. It is noteworthy that the isotope effects due to the different chlorine isotopes are observed in the ^{19}F NMR spectrum of CDFClBr as well. This was taken into account for the fitting. Indeed, the line shapes were fitted as the sum of two ponderated functions of the type of eq 9 corresponding to the signals of CDF^{35}ClBr and CDF^{37}ClBr, with an IECS of 3.1 ppb. Respective values of $T_q = 0.35$ s and $T_q = 0.134$ s were found for the quadrupolar relaxation time of the free and the two complexed signals. ^{2}H relaxation is more efficient for the bound guest molecule.

Determination of the Correlation Time τ_C from Deuterium Quadrupolar Relaxation Times

Considering again the case of isotropic tumbling, the quadrupolar relaxation time T_q is related to the correlation time τ_C

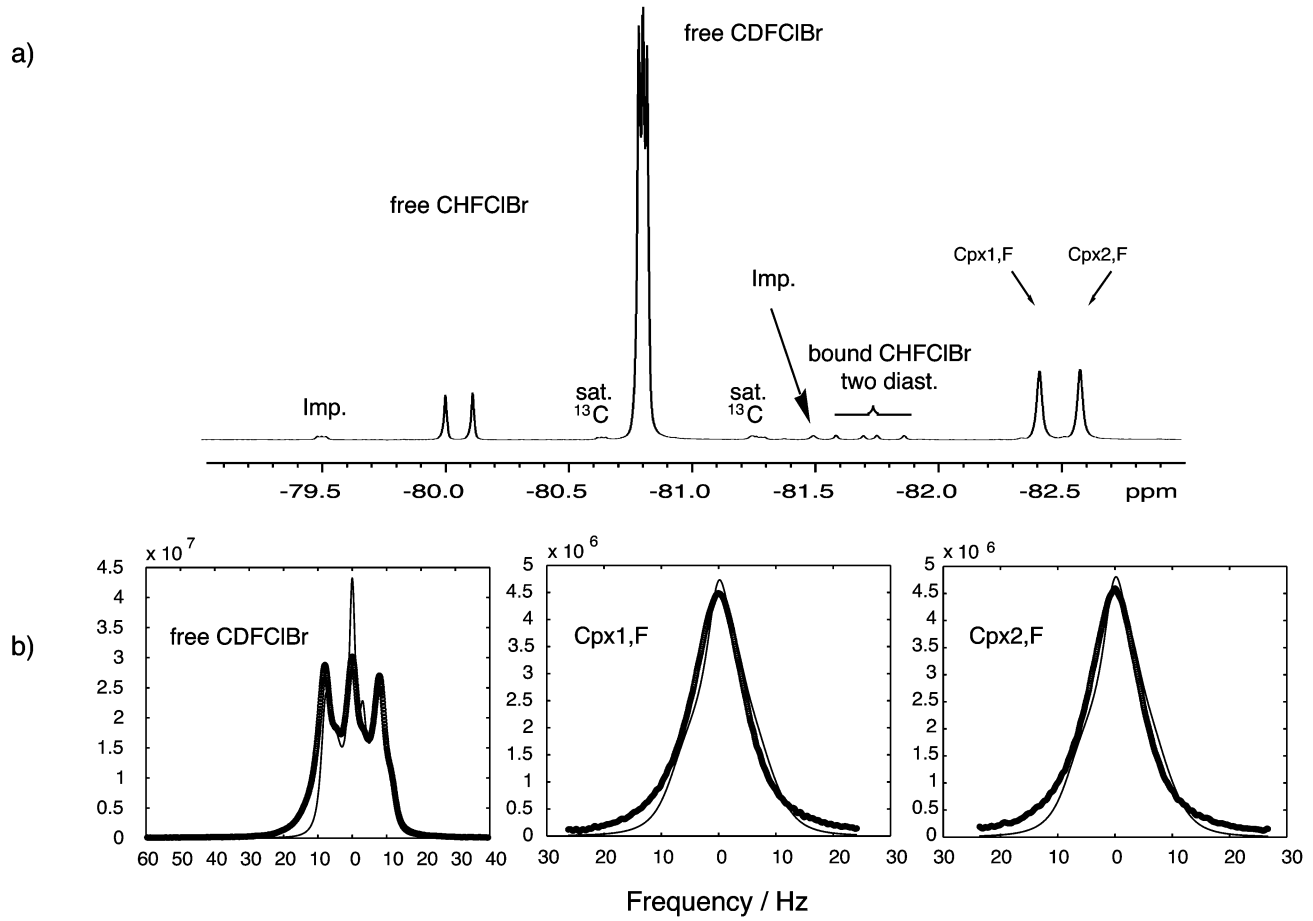

Figure 7. Complexation of (±)-CDFClBr by (±)-cryptophane-E-$(SCH_3)_6$ at 298 K. (a) Entire ^{19}F NMR spectrum at 11.74 T. (b) Expansion on the different fluorine lines of the free and complexed CDFClBr (thin lines) and best fitting of each line shape (thick line) according to eq 9.

of the molecule according to

$$\frac{1}{T_q} = \frac{3}{8}\chi^2\tau_C \qquad (10)$$

The factor χ is known to be constant for a series of molecules having the same type of C−D bond. Therefore, taking for χ a common value of 170 kHz found for a sp^3 C−D bond,[19] τ_C values of 0.27 and 0.69 ns were found for the free and the bound CDFClBr, respectively. This is in perfect agreement with the values obtained from the fluorine-proton cross-correlated relaxation rates of CHFClBr.

Conclusions

We have shown that thiomethylated cryptophanes such as **4** are important chiral hosts for the future enantiomeric excess determination of optically resolved halogenomethanes such as CHFClI (work in progress).

Moreover, the dynamics of complexed CHFClBr and CDFClBr in cryptophane E-$(SCH_3)_6$ were examined by means of spin relaxation measurements. Using two different and independent experimental relaxation parameters, the ^{19}F−^{1}H CSA-DD cross-correlated relaxation time for CHFClBr and the deuterium quadrupolar relaxation time for CDFClBr, we obtained consistent values for the correlation time τ_C of the guest. These values are also in very good agreement with Kowalewski's results for the complexation of $CHCl_3$ by cryptophane-E.

In summary, we have shown that fluorine can be used as a sensitive probe to investigate the molecular motion of a fluorinated guest inside a cavity, by spin relaxation measurements. The next step of our work will be to use similar relaxation methods to determine the kinetic constants of a faster complexation process, as observed in the case of CHFClBr or CHFClI with cryptophane-E.

Experimental Section

[D_2]tetrachloroethane was purchased from Eurisotop. Bromochlorofluoromethane and bromochlorodeuteriofluoromethane were prepared according to the literature.[21] The sample consisting of (±)-cryptophane-E and (±)-CHFClBr was prepared by mixing 8.1 mg (8.64 μmol) of (±)-**3** and 1.1 μL (14.7 μmol) of (±)-**5** in 0.7 mL of $C_2D_2Cl_4$. The sample consisting of (±)-cryptophane-E-$(SCH_3)_6$ and (±)-CHFClBr was prepared by mixing 13 mg (12.6 μmol) of (±)-**4** and 3.2 μL (41.6 μmol) of (±)-**5** in 0.7 mL of $C_2D_2Cl_4$. The sample consisting of (±)-cryptophane-E-$(SCH_3)_6$ and (±)-CDFClBr was prepared by mixing 11.6 mg (11.2 μmol) of (±)-**4** and 1 μL (12.91 μmol) of (±)-**6** in 0.7 mL of $C_2D_2Cl_4$. Each sample was degassed using the freeze−pump−thaw procedure (three times) and flame-sealed. Each experiment was performed twice.

The NMR experiments were performed on a Varian Unity+ (11.74 T) and a Bruker DPX200 (4.7 T) spectrometer. All experiments were performed at 25 °C using the standard temperature controller. On the Varian, a standard ^{1}H/^{13}C/^{15}N triple-resonance probe was used. The Bruker spectrometer was equipped with a QNP probe head. On both spectrometers, the ^{19}F experiments were performed by tuning the proton channel to the fluorine frequency (468.4 and 188.2 MHz, respectively). For the inversion−recovery experiments, the $\pi/2$ pulse was 8.2

μs at 468.4 MHz and 8.4 μs at 188.2 MHz. The relaxation delay τ was set to 15 different values between 37.5 ms and 9.6 s. For each τ, 260 transients with a recovery delay of 14 s were added up.

The least-squares fittings of the relaxation curves and the fluorine line shape according to eqs 4, 5, and 10 were performed with the commercial software Matlab.[22]

Acknowledgment. Many thanks to Anne Lesage and Luminita Duma for their technical support. Thanks to Delphine Humilière for her gift of cryptophane-E-$(SCH_3)_6$. We are very grateful to Claude Béguin, Anil Kumar, and Bernhard Brutscher for helpful discussions.

References and Notes

(1) Collet, A.; Dutasta, J.-P.; Lozach, B.; Canceill, J. *Top. Curr. Chem.* **1993**, *165*, 103−129.

(2) Garel, L.; Lozach, B.; Dutasta, J.-P.; Collet, A. *J. Am. Chem. Soc.* **1993**, *115*, 11652−11653.

(3) Garel, L.; Dutasta, J.-P.; Collet, A. *Angew. Chem., Int. Ed. Engl.* **1993**, *32*, 1169−1171.

(4) (a) Bartik, K.; Luhmer, M.; Dutasta, J.-P.; Collet, A.; Reisse, J. *J. Am. Chem. Soc.* **1998**, *120*, 784−791. (b) Brotin, T.; Devic, T.; Lesage, A.; Emsley, L.; Collet, A. *Chem. Eur. J.* **2001**, *7*, 1561−1573. (c) Brotin, T.; Lesage, A.; Emsley, L.; Collet, A. *J. Am. Chem. Soc.* **2000**, *122*, 1171−1174.

(5) (a) Costante-Crassous, J.; Marrone, T. J.; Briggs, J. M.; McCammon, A.; Collet, A. *J. Am. Chem. Soc.* **1997**, *119*, 3818−3823. (b) Kirchhoff, P. D.; Bass, M. B.; Hanks, B. A.; Briggs, J. M.; McCammon, A.; Collet, A. *J. Am. Chem. Soc.* **1996**, *118*, 3237−3246. (c) Kirchhoff, P. D.; Dutasta, J.-P.; Collet, A.; McCammon, A. *J. Am. Chem. Soc.* **1997**, *119*, 8015−8022.

(6) Varnek, A.; Helissen, S.; Wipff, G.; Collet, A. *J. Comput. Chem.* **1998**, *19*, 820−832.

(7) Lang, J.; Dechter, J. J.; Effemey, M.; Kowalewski, J. *J. Am. Chem. Soc.* **2001**, *123*, 7852−7858.

(8) Tosner, Z.; Lang, J.; Sandström, D.; Petrov, O.; Kowalewski, J. *J. Phys. Chem. A* **2002**, *106*, 8870−8875.

(9) Gabard, J.; Collet, A. *J. Chem. Soc., Chem. Commun.* **1981**, 1137−1139.

(10) Canceill, J.; Lacombe L.; Collet A. *J. Am. Chem. Soc.* **1985**, *107*, 6993−6996.

(11) Garcia, C.; Humilière D.; Riva, N.; Collet, A.; Dutasta, J.-P. *Org. Bioorg. Chem.* **2003**, *1*, 2207−2216.

(12) The complexation studies were carried out on the racemic forms, and therefore, we could not assign properly the signals to the configuration of the two diastereomeric complexes. For commodity, the down-shielded doublet is named Cpx1,H and the up-shielded doublet Cpx2,H in ^{1}H NMR. The terms Cpx1,F and Cpx2,F are used in the case of ^{19}F NMR.

(13) (a) Sergeyev, N. M.; Sandors, P.; Sergeyeva, N.; Raynes, W. *J. Magn. Res., Series A* **1995**, *115*, 174−182. (b) Tordeux, M.; Wakselman, C.; Jarjayes, O.; Béguin, C. G. *Magn. Res. Chem.* **2001**, *39*, 301−310.

(14) Ernst, R. R.; Bodenhausen, G.; Wokaun, A. *Principles of Nuclear Magnetic Resonance in One and Two Dimensions*; Clarendon Press: Oxford, 1997.

(15) (a) Dorai, K.; Kumar, A. *Chem. Phys. Lett.* **2001**, *335*, 176−182. (b) Kumar, A.; Christy Rani Grace, R.; Madhu, P. K. *Prog. NMR Spectrosc.* **2000**, *37*, 191−319.

(16) Brutscher, B. *Concepts Magn. Reson.* **2000**, *12*, 207−229.

(17) Lipari, G.; Szabo, A. *J. Am. Chem. Soc.* **1982,** *104*, 4546−4559.

(18) (a) Brévard, C.; Kintzinger, J. P.; Lehn, J. M. *Tetrahedron* **1972**, *28*, 2429−2445. (b) Brévard, C.; Kintzinger, J. P.; Lehn, J. M. *Tetrahedron* **1972**, *28*, 2447−2460. (c) Brévard, C.; Lehn, J. M. *J. Am. Chem. Soc.* **1970**, *92*, 4987−4989. (d) Brévard, C.; Kintzinger, J. P.; Lehn, J. M. *Chem. Commun.* **1969**, 1193−1195.

(19) (a) Béguin, C. G.; Dupeyre, R. *C. R. Acad. Sci. Paris* **1971**, *273*, 1658−1661. (b) Béguin, C. G.; Dupeyre, R. *J. Magn. Reson.* **1981**, *44*, 294−313.

(20) Abragam, A. *The principles of Nuclear Magnetism*; Clarendon Press: Oxford, 1961.

(21) Doyle, T. R.; Vogl, O. *J. Am. Chem. Soc.* **1989,** *111*, 8510−8511.

(22) Matlab; The Mathworks, Inc.: Natick, MA.